



STRONG GROUND MOTION SIMULATION FOR RECENT EARTHQUAKES IN CHINA

GX. Wang⁽¹⁾, YN. Li⁽²⁾

⁽¹⁾ Professor, Institute of Earthquake Engineering, Dalian University of Technology, gxwang@dlut.edu.cn

⁽²⁾ Doctor, Institute of Earthquake Engineering, Dalian University of Technology, liyananren@gmail.com

Abstract

Stochastic point source method with its extended version finite fault method is widely used to simulate strong ground motions around the world. In view of the limitation of uniform slip distribution in point source method with effective distance (R_{EFF}), a new modified version of the stochastic method based on a proposed equivalent distance (R_{EQL}) measure is proposed. To incorporate the effect of heterogeneous slip distribution on previous modified point source method, the uneven slip values are first transformed to distance value assigned to sub-faults, and then solved for the comprehensive distance R_{EQL} iteratively to the path spreading functions. At last, the ratio of total spectrum Y for non-uniform and uniform slip distributions can be obtained from the path term in Y spectrum.

The new modified method is used to simulate two recent earthquakes in China, The Wenchuan ($M_w=8.3$, 12 May, 2008) and Ludian ($M_w=6.2$, 3 August, 2014) earthquakes. For Wenchuan earthquake, envelop method is combined with the new present method to simulate the waveform of the acceleration time history because its fault is relatively long. Simulation results for 6 stations around the fault indicate that the present method could simulate the direction and hanging wall effect of strong earthquake. For Ludian earthquakes, parameters are investigated by analyzing 69 recorded accelerograms. Comparisons between observed and simulated parameters, such as peak ground acceleration (PGA) against R_{EQL} , waveforms and pseudo-spectral acceleration (PSA), indicate that the simulation parameters and results for Ludian earthquake ($M_w 6.2$, 3 August, 2014, China) are quite acceptable. Furthermore, the ShakeMaps of Ludian in terms of PGA simulated by the present method and finite-fault method are further compared with intensity map published by China Earthquake Administration, which also confirms the validity of the new simulation procedure for the purpose of regional strong ground motion estimation. The simulation results also indicate that input parameters for the two earthquakes are similar. The proposed method has the advantage of simple and efficient on computation efficiency.

Keywords: point-source method; finite-fault method; equivalent distance; Wenchuan earthquake; Ludian earthquake



1. Introduction

The Wenchuan ($M_w=8.3$, 12 May, 2008) and Ludian ($M_w=6.2$, 3 August, 2014) earthquakes are two recent strong earthquakes located in northeast China, where temblors are prone to happen. The former one resulted in 70 thousand people dead while the latter one affected more than 1 million people. The direct economic losses of the two earthquakes are as high as 850 billion yuan. The main common reason for the casualties during the earthquakes is due to building collapse because most of the buildings in these regions are masonry and poorly designed concrete structures.

Normally, strong ground motion with high-frequency (greater than 1 Hz) are generally required by engineers as the inputs for structural nonlinear dynamic analysis in seismic design, especially for those who are engaged in performance-based seismic design, and the recorded accelerograms are the most popular used in practice because they provide data basic for the understanding of source processes^[1]. But the quantity of high-quality recorded ground motions is very limited and sometimes it may difficult to meet the requirement for special analysis conditions, such problems are very typical in most of regions in the world due to lack of, even without strong ground motion recordings. To solve such problems, amplitude scaling and spectral matching with typical recordings (e.g. records from Loma Prieta, Northridge, Chi-Chi earthquakes and so on) are the widely used methods to generate enough numbers of ground motions that can be representative of various analysis conditions. However, the characteristics of the ground motion recordings may be modified so that they are not consistent with the physical conditions in terms of earthquake source mechanism and local geology, and the results from these operations could have the features different from those of the real recordings^[2]. Therefore, it is necessary to simulate different strong ground motions that can involve and embody the earthquake physical conditions and characteristics of the actual ground motion recordings.

Stochastic method is a good choice for such purpose. It simulates ground motions based on modified Gaussian white noise by considering the source mechanism, propagation characteristics and site effect through empirical regression. It is typically thought that stochastic method performs well only in prediction ground motions in high-frequency range. However, Motazedian and Atkinson^[3] point that finite-fault stochastic and hybrid methods could perform equally well across a broad range of frequencies from 0.1 to 20 Hz, according to comparisons made by Hartzell et al^[4].

Stochastic point-source method (hereafter, PS method) is first proposed by Boore^[1] based on far-field Brune-model source spectrum^[5-10]. Then, Beresnev and Atkinson^[11] followed Hartzell's^[12] idea and subdivided a large fault into N sub-faults and each sub-fault being considered as a small point source. The ground motions of sub-faults, each of which is calculated by the stochastic PS method, are summed with a proper time delay in time domain. This is the so-called stochastic finite-fault source method (hereafter, FF method). These methods have been successfully applied to many regions all over the world^[13-17].

Although some simplifications are applied to aforementioned stochastic method, it considers both deterministic and random aspects of ground motion shaking^[10]. The deterministic aspects are that frequency contents can be scaled according to source parameters, such as magnitude, distance as well as high- and low-frequency filters. The stochastic aspects are specified by the Gaussian white noise that is filtered and windowed by appropriate spectrum. Those deterministic parameters are empirically analyzed from large quantities of real recordings. In addition, stochastic method is suitable for engineering application since it produce ground motions that have frequencies within the interest of engineering with high computation speed.

In this study, the Wenchuan and Ludian earthquake are simulated by a new improved PS method. Its computational speed is much faster than deterministic or hybrid method and even FF method. To be specific, a new variable called equivalent distance (R_{EQL}) is proposed. R_{EQL} is a comprehensive distance that determined by both the sub-fault distance and sub-fault slip distributions. The simulations for the two earthquakes on one hand will help to investigate the parameters for these regions, and on the other hand demonstrate that the proposed method is effective and practical.



2. Simulation Methodology

In stochastic PS method, the total spectrum $Y(M_0, R, f)$ used to normalize the spectrum amplitude of filtered and windowed Gaussian white noise, can be separated into several contributions from earthquake source (E), path (P), site (G), type of motion (I), and sometimes low frequency cutter (L), thus:

$$Y(M_0, R, f) = E(M_0, f)P(R, f)G(f)I(f)L(f) \quad (1)$$

where M_0 is the seismic moment, R is distance between site and epicenter and f is frequency in Hz. Detailed information can be found in references [18] and [3].

FF method is the extension of PS method. But researchers found that the results of PS method and FF source method are not the same even for a small earthquake at a substantial distance (see reference [19]). Boore^[20] first discussed this inconformity of the two methods and proposed a modification to PS method: replacing closest distance (R_{CD}) with a so-called effective distance measure (R_{EFF}), which is given by:

$$P(R_{EFF}, f_Q) = [\sum_{i=1}^N P(R_i, f_Q)^2 / N]^{1/2} \quad (2)$$

where N is the total number of sub-faults, R_i is the distance from the site to i th sub-fault and f_Q is set as 10 Hz because it is found that 10 is of a best fit. The right side is calculated and then R_{EFF} is found iteratively such that the left side of the equation equals the right side of the equation. Eq. (2) tries to adopt a comprehensive average value of distances between sub-faults and site for calculation.

In the present study, a more flexible and practical distance R_{EQL} is proposed according to theory of R_{EFF} . The advantage of R_{EQL} method is that it not only considers the geometric dimension of fault but also the heterogeneous slip distribution of the fault, which is closer to actual situation. First consider a relative non-uniform slip distribution $SR^*(i, j)$, i.e., slip matrix divided by sum of all matrix elements. Since M_{0ij} is determined by the slip value of sub-faults, source term E_{ij} will be different with each other according to PS method, which is equal with each other under relative uniform slip distribution $SR^1(i, j)$. Since R_{EFF} can catch the comprehensive average value of distances between sub-faults, it is possible to convert the ratio of seismic moment to the ratio of distance between sub-fault and site with the following equations:

$$K(i, j) = S_R^*(i, j) / S_R^1(i, j) \quad (3)$$

$$P(R_{i,j}^*, f_Q) = K(i, j) \times P(R_{i,j}^1, f_Q) \quad (4)$$

where $K(i, j)$ is the ratio of non-uniform to uniform slip distribution. R_{ij}^* and R_{ij}^1 are distance from site to i, j th sub-fault under non-uniform and uniform slip distribution respectively. Then, with Eq (4), we can get a new set of distances and the slip distribution become uniform under these distances. The newly obtained distances are not sufficient to get a final distance for PS simulation. It is found that results of simulation under non-uniform slip distribution are β times that under uniform slip distribution. The ratio β is calculated with Eq (5) - (7):

$$P(R_{EFF}^1, f_Q) = [\sum_{i=1}^N P(R_i^1, f_Q)^2 / N]^{1/2} \quad (5)$$

$$P(R_{EQL}, f_Q) = [\sum_{i=1}^N P(R_{i,j}^*, f_Q)^2 / N]^{1/2} \quad (6)$$

$$\beta = P(R_{EQL}, f_Q) / P(R_{EFF}^1, f_Q) \quad (7)$$

where R_{EQL} and R_{EFF}^1 are equivalent distance and effective distance under non-uniform and uniform slip distribution, respectively. At last, β is the critical parameter in the usage of modified PS method. Total spectrum Y_{EQL} for simulated motion is multiplied by β .

3. Simulation of Earthquakes

3.1 Wenchuan earthquake

Wenchuan earthquake occurred in Wenchuan county of Sichuan province and has long rupture time. In this section, waveform envelope function proposed by Pacor^[21] is used rather than Saragoni window function^[22] used in PS method, which is suitable for fault that is long and will not be described here considering the length of the paper. Fig.1 shows the fault slip distribution inversed by Yagi^[23] and simulated sites of Wenchuan earthquake. In the simulation, slip distribution is further refined according to the size of sub-faults. In order to reflect the characteristic of near-fault ground motions, 6 stations are selected around the fault including foot and hanging wall stations, as shown in the right graph of Fig.1. Table 1 is the input parameters according to the research of Yan Yu^[24].

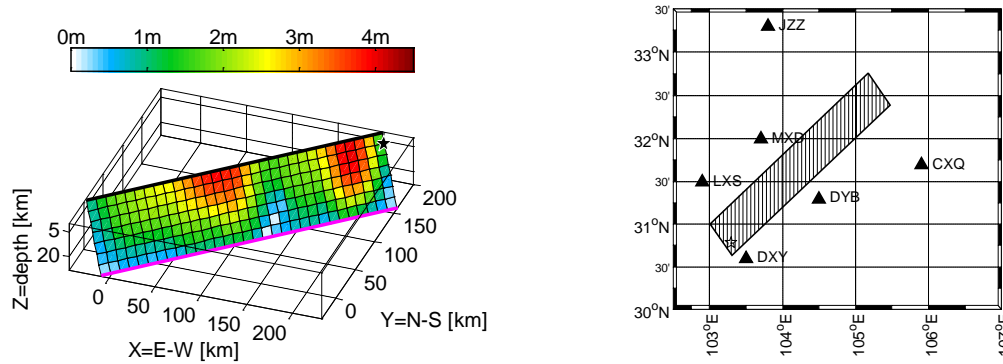


Fig. 1 – Slip distribution and simulated stations of Wenchuan earthquake

Table 1 – Input parameters for Wenchuan earthquake

Item	Parameter	Item	Parameter
Strike and dip	231°, 32°	Quality factor Q	$303 \times f^{0.39}$
Fault dimension (km × km)	320×60	Rupture velocity (km/s)	3.0
Sub-fault dimension (km × km)	2×2	High frequency attenuation κ_0	0.003
Moment Magnitude	8.3	Geometry spreading $Z(R)$	$1/R^{1.3}$ $R \leq 70\text{km}$
Stress drop (bar)	200		$0.07/R^{0.5}$ $70 \leq R \leq 140\text{km}$
Shear wave velocity (km/s)	3.7		$0.1/R^{0.5}$ $R > 140\text{km}$

Fig. 2 shows the simulation of the 6 stations around the fault. For each station, the figure displays pseudo-spectral acceleration (PSA), recorded, simulated acceleration time history and normalized envelope of the ground motion. In general, the PSA and waveform of simulated ground motion conform to the recorded one, indicating that the input parameters in Table 1 are reasonable. Station CXQ and DYC are in the front of rupture direction, so their duration appears to be short, while the station DXY and LXS have long duration as they are in the back of rupture direction. For footwall stations DXY, DYC and CXQ, their PGA is smaller than hanging wall stations LXS, MXD, which demonstrates that the present method could simulate hanging wall effect.

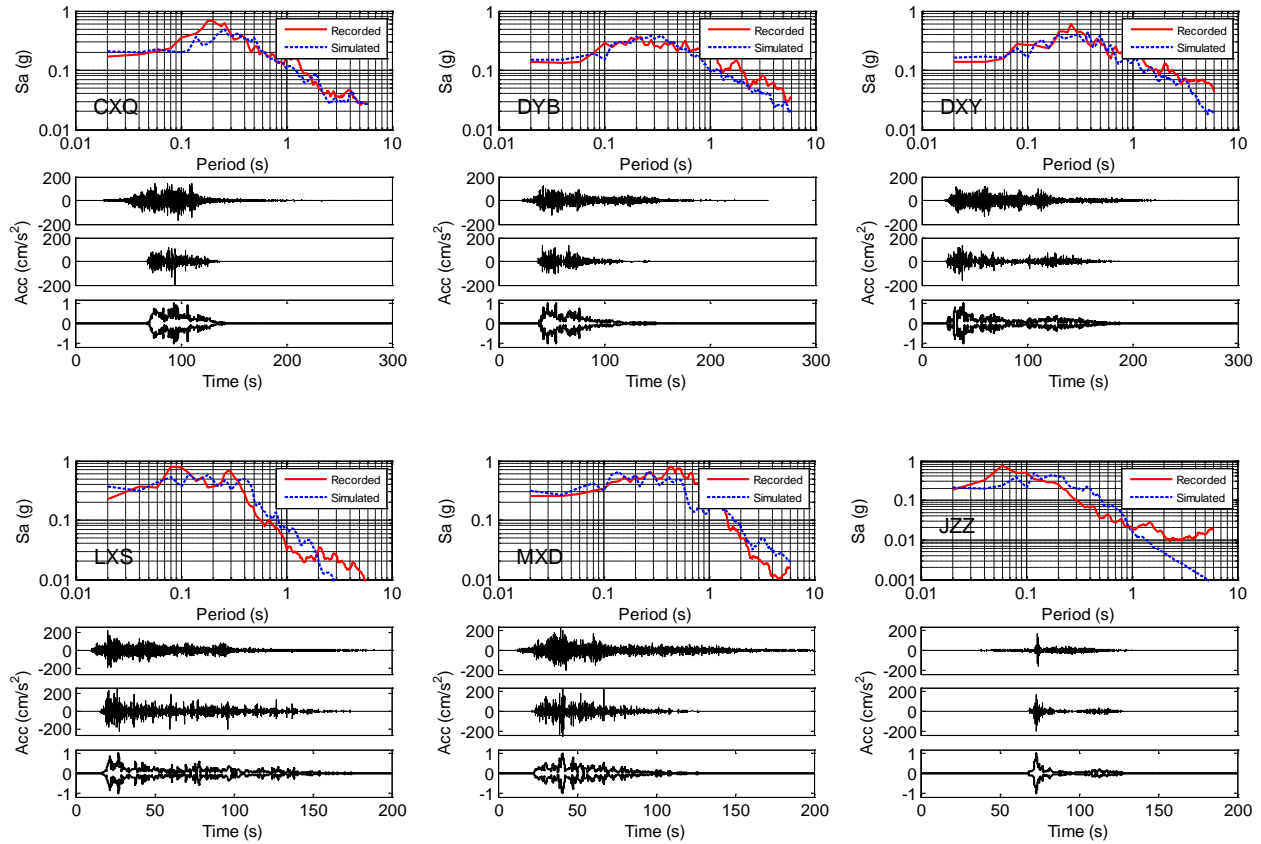


Fig. 2 – Simulation of Wenchuan earthquake for 6 stations

3.2 Ludian earthquake

Ludian earthquake is located in the junction of Yunnan, Sichuan and Guizhou provinces. The fault geometry, hypocenter and slip distribution follows the results inversed by Institute of Geology and Geophysics of Chinese Academy of Sciences (IGGCAS), as shown in Fig.3. The model region covers the total area within about 300 km×300 km, and there are 69 recording sites around. Fig.3 shows a map view of the rupture surface and recording sites. The fault is 75 km long and has a down-dip width of 56 km. The strike is 162°, dip is 83°, and the average rake is 6°. Sub-faults size is set to be 2 km × 2km. The seismic moment is 2.2387×10^{18} N•m, giving a moment magnitude of 6.2. Table 2 is the input parameters determined according to the data recorded by the 69 stations because there is little references for this region.

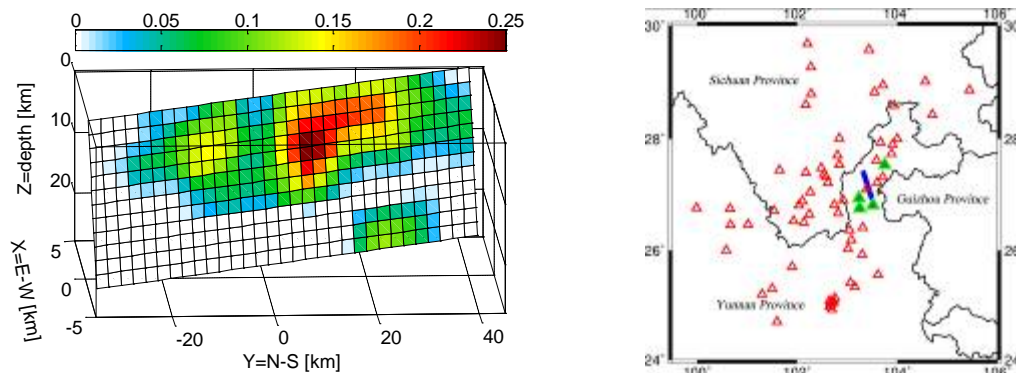


Fig. 3 – Slip distribution and stations of Ludian earthquake

Table 2 – Input parameters for Ludian earthquake

Item	Parameter	Item	Parameter
Strike and dip	162°, 83°	Quality factor Q	$303 \times f^{0.39}$
Fault dimension (km × km)	75×56	Rupture velocity (km/s)	3.0
Sub-fault dimension (km × km)	2×2	High frequency attenuation κ_0	0.004
Moment Magnitude	6.2	Geometry spreading $Z(R)$	$1/R^{1.0}$ $R \leq 70\text{km}$
Stress drop (bar)	50		$0.014/R^{0.0}$ $70 \leq R \leq 140\text{km}$
Shear wave velocity (km/s)	3.7		$0.014/R^{0.5}$ $R > 140\text{km}$

Fig.4 compares observed and simulated ground-acceleration waveforms and pseudo-spectral acceleration (PSA) at four sites. These sites are indicated on the map shown in Fig.3 and were chosen as a representative for near fault sites. In general the amplitude, duration and frequency content of the observed wave forms are matched reasonably well by the simulated for these sites. Although stochastic method performs not as good as broadband method at low frequency ranges (53QJX and 53QQC), it can be capable to simulate low frequency motions even lower than 1Hz (53HYC and 53ZJA). The most important parameters to control the frequency content of simulated motions are κ_0 and f_{cut} . For the Ludian earthquake, κ_0 is from 0.03 to 0.05, while the f_{cut} is from 0 to 0.9.

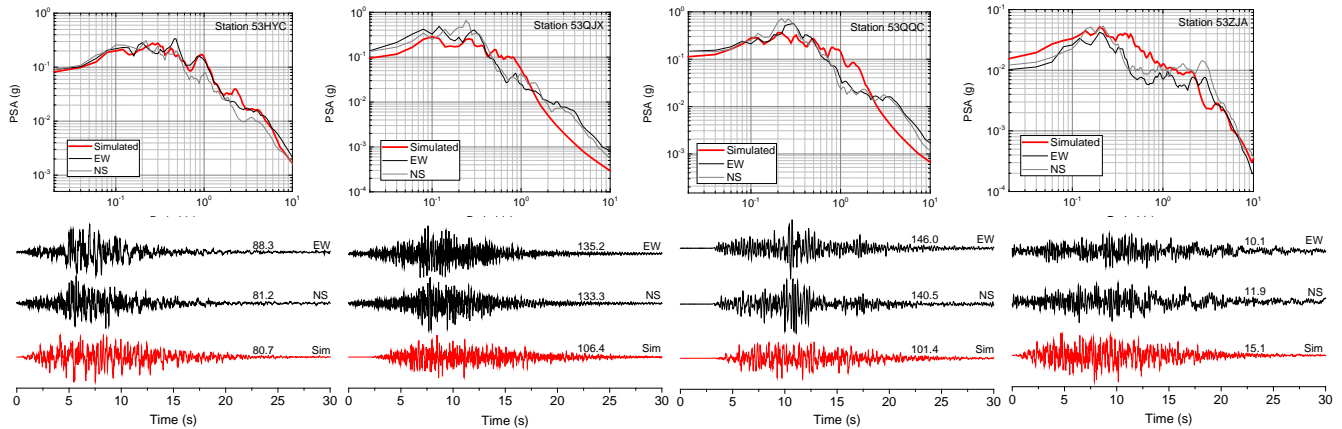


Fig. 4 – Comparison of recorded and simulated PSA and acceleration waveforms at four selected sites for the Ludian earthquake.

Fig.5 further simulated the ShakeMaps of Ludian earthquake in terms of PGA by the present method and EXSIM, and then are compared with the intensity map. Intensity data are extracted from the map published by China Earthquake Administration (CEA). For simulated PGA field, the grid of sites covers a region that extends in latitude from 24.4° N to 30° N and in longitude from 100.6° E to 106.4° E with grid length of 0.2°. Besides, grid spacing is denser (0.1°) for the region around the fault, i.e. in latitude from 26.5° N to 27.8° N and in longitude from 102.8° E to 104° E. Thus, totally 990 geometric nodes are set as assumed stations for Ludian area. Note that the station specific parameters, such as $A(f)$, κ_0 and f_{cut} , are averaged for every nodes. Contour values that smaller than 0.02g are ignored as the 0.02g contour is close to the boundary of intensity VI. The results, on the one hand, show that the present method reached good agreement with EXSIM in the PGA prediction for regions, which can be compared by the last two panels in Fig.5. On the other hand, simulated ShakeMaps have captured the main feature of the intensity map. They are all ellipse with a northwest-southeast long axis. The PGA contours of 0.2g, 0.1g and 0.02g are corresponding to intensity VI, VII, VIII. It is worth noting that the

intensity map is obtained by investigating damage to buildings, damage to natural landscape and sometimes casualties. The shape and value of intensity contours are influenced by sampling quantities and are subjective. Therefore, the simulated ShakeMaps is hard to be exactly the same with intensity map. Also, the ShakeMaps are similar with those published by USGS. According to the poster on USGS, the peak acceleration is no more than 0.22 g and attenuates very quickly to below 0.028 g.

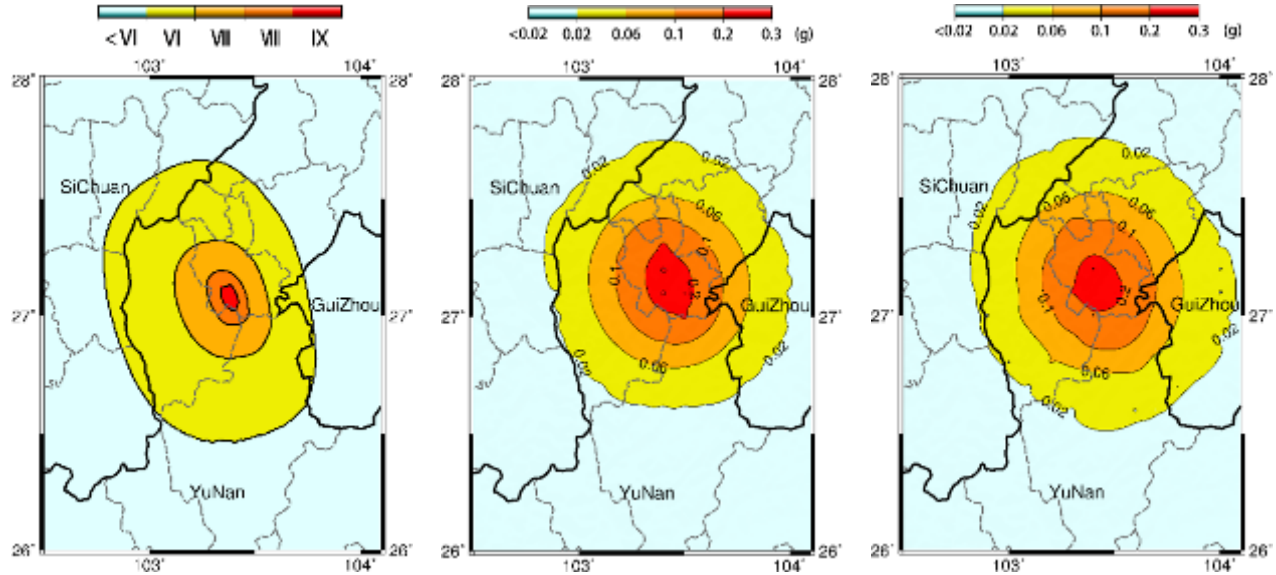


Fig. 5 – Comparison of published intensity map (a), simulated ShakeMaps by present method (b) and EXSIM (c) for Ludian earthquake. Parameters for all models are the same.

4. Conclusion

The stochastic PS method with R_{EFF} is reviewed and modified herein to include uneven slip distribution on fault plane. The R_{EFF} distance measure is replaced by R_{EQL} , which is a comprehensive distance that determined by both the sub-fault distance and sub-fault slip distributions. The R_{EQL} combines both the advantage of PS and FF method and has wider range of application.

The new method is used to simulate the 2008 Wenchuan earthquake and 2014 Ludian earthquake. For the Wenchuan earthquake, evenlop technique is combined to simulate the waveform of near-fault sites, which is suitable for earthquake that has long fault. A stress drop of 200 bar and $Q(f)=303f^{0.39}$ agree well with real ground motions. The duration and hanging wall effect can be simulated by the present method. For the Ludian earthquake, a stress drop of 50 bar and $Q(f)=303f^{0.39}$ agree well with real ground motions. The contour maps generated for Ludian earthquakes above showing the simulated PGA field is in general consistent with the intensity maps published by CEA. The fact that PGA contours are greatly influenced by the slip distributions on fault plane conforms the assumption that sub-fault with high slip values causes strong motions around. Also note that the quality of inversed slip distribution is the dominant factor that could affect the near-fault PGA field.

5. Acknowledgements

The research described in this paper was financially supported by the National Natural Science Foundation of China under Grant No. 51121005 and 51378092. We wish to thank Mr. David M. Boore for the guidance on the use of SMSIM and his help with basic idea of finite-fault method.



6. Copyrights

16WCEE-IAEE 2016 reserves the copyright for the published proceedings. Authors will have the right to use content of the published paper in part or in full for their own work. Authors who use previously published data and illustrations must acknowledge the source in the figure captions.

7. References

- [1] Boore DM (1983): Stochastic simulation of high-frequency ground motions based on seismological models of the radiated spectra. *Bulletin of the Seismological Society of America*, 73(6A), 1865-1894.
- [2] Luco N, Bazzurro P (2007): Does amplitude scaling of ground motion records result in biased nonlinear structural drift responses?. *Earthquake Engineering & Structural Dynamics*, 36(13), 1813-1835.
- [3] Motazedian D, Atkinson GM (2005): Stochastic finite-fault modeling based on a dynamic corner frequency. *Bulletin of the Seismological Society of America*, 95(3), 995-1010.
- [4] Hartzell S, Harmsen S, Frankel A, Larsen S (1999): Calculation of broadband time histories of ground motion: Comparison of methods and validation using strong-ground motion from the 1994 Northridge earthquake. *Bulletin of the Seismological Society of America*, 89(6), 1484-1504.
- [5] Brune JN (1970): Tectonic stress and the spectra of seismic shear waves from earthquakes. *Journal of geophysical research*, 75(26), 4997-5009.
- [6] Hanks TC, McGuire RK (1981): The character of high-frequency strong ground motion. *Bulletin of the Seismological Society of America*, 71(6), 2071-2095
- [7] Atkinson GM, Boore DM (1995): Ground-motion relations for eastern North America. *Bulletin of the Seismological Society of America*, 85(1), 17-30.
- [8] Atkinson GM, Boore DM (1997): Some comparisons between recent ground-motion relations. *Seismological Research Letters*, 68(1), 24-40.
- [9] Toro GR, Abrahamson NA, Schneider JF (1997): Model of strong ground motions from earthquakes in central and eastern North America: best estimates and uncertainties. *Seismological Research Letters*, 68(1), 41-57
- [10] Atkinson GM, Assatourians K, Boore DM, Campbell K, Motazedian D (2009), A guide to differences between stochastic point-source and stochastic finite-fault simulations. *Bulletin of the Seismological Society of America*, 99(6), 3192-3201.
- [11] Beresnev IA, Atkinson GM (1997): Modeling finite-fault radiation from the ω spectrum. *Bulletin of the Seismological Society of America*, 87(1), 67-84.
- [12] Hartzell SH (1978): Earthquake aftershocks as Green's functions. *Geophysical Research Letters*, 5(1), 1-4.
- [13] Ou GB, Herrmann RB (1990): A statistical model for ground motion produced by earthquakes at local and regional distances. *Bulletin of the Seismological Society of America*, 80(6A), 1397-1417.
- [14] Beresnev Igor A, Atkinson GM (1998b): Stochastic finite-fault modeling of ground motions from the 1994 Northridge, California, earthquake. I. Validation on rock sites. *Bulletin of the Seismological Society of America*, 88(6), 1392-1401.
- [15] Atkinson GM, Boore DM (2006): Earthquake ground-motion prediction equations for eastern North America. *Bulletin of the Seismological Society of America*, 96(6), 2181-2205.
- [16] Kanth SR, Iyengar RN (2007): Estimation of seismic spectral acceleration in Peninsular India. *Journal of Earth System Science*, 116(3), 199-214.
- [17] Edwards B, Fäh D (2013): A stochastic ground - motion model for Switzerland. *Bulletin of the Seismological Society of America*, 103(1), 78-98.
- [18] Boore DM (2003): Simulation of ground motion using the stochastic method. *Pure and applied geophysics*, 160(3-4), 635-676.



- [19] Campbell KW (2008): Hybrid empirical ground motion model for PGA and 5% damped linear elastic response spectra from shallow crustal earthquakes in stable continental regions: Example for eastern North America. *Proceedings of the 14th World Conference on Earthquake Engineering*, Beijing, China, October.
- [20] Boore DM (2009): Comparing stochastic point-source and finite-source ground-motion simulations: SMSIM and EXSIM. *Bulletin of the Seismological Society of America*, 99(6), 3202-3216.
- [21] Pacor F, Cultrera G, Mendez A, Cocco, M (2005): Finite fault modeling of strong ground motions using a hybrid deterministic–stochastic approach. *Bulletin of the Seismological Society of America*, 95(1), 225-240.
- [22] Rodolfo Saragoni G, Hart GC (1973): Simulation of artificial earthquakes. *Earthquake Engineering & Structural Dynamics*, 2(3), 249-267.
- [23] Yagi Y, Nishimura N, Kasahara A (2012): Source process of the 12 May 2008 Wenchuan, China, earthquake determined by waveform inversion of teleseismic body waves with a data covariance matrix[J]. *Earth Planets Space*, 64(7), e13-e16.
- [24] Yu,Y (2012): Empirical estimate model for ground motion of Wenchuan earthquake zone (in Chinese). Institute of Engineering Mechanics, China Earthquake Administration, Harbin.